To cite this article: ZHOU L, QIU Z Q, YUAN Y S, et al. Vortex-induced vibration of cylinder under sub-critical Reynolds number[J/OL]. Chinese Journal of Ship Research, 2022, 17(3). http://www.ship-research.com/en/article/doi/10.19693/j.issn.1673-3185.02694.

DOI: 10.19693/j.issn.1673-3185.02694

Vortex-induced vibration of cylinder under sub-critical Reynolds numbers

ZHOU Li, QIU Zhongqiu, YUAN Yashuai, ZONG Zhi*

School of Naval Architecture, Dalian University of Technology, Dalian 116024, China

Abstract: [**Objective**] In order to accurately predict the amplitude response of the vortex-induced vibration (VIV) of a cylinder under sub-critical Reynolds numbers, a numerical simulation is proposed to establish the relationship between a lift coefficient and amplitude ratio (*Cl*-*A*/*D*) of the cylinder under forced vibration. [**Methods**] On the basis of the Realizable *k*-*ε* model, a two-dimensional numerical simulation is carried out on the forced vibration of the cylinder by using the finite volume method. The lift coefficient curves under different amplitude ratios with an excitation frequency ratio f_e/f_n=1 are obtained through calculation. The lift coefficient corresponding to the maximum vibration velocity of the cylinder is then selected to establish the *Cl*-*A*/*D* curve. [**Results**] The results show that the overall trend of the *Cl*-*A*/*D* curve is in good agreement with the prediction results of SHEAR7. At the same time, it is found that the zero-lift coefficient points under different excitation frequency ratios are all located near *A*/*D* = 0.8, and the wake vortex shedding mode changes around *A*/*D*=0.8 from P+S to 2P (P represents a pair of vortex shedding with opposite rotation directions, and S represents a single vortex shedding). In the VIV experiment of a cylinder, the maximum amplitude when a locking state is reached is around 0.8 *D*. [**Conclusions**] The amplitude ratio corresponding to the zero-lift coefficient of the *Cl*-*A*/*D* curve of the cylinder under forced vibration and sub-critical Reynolds number is consistent with the maximum response amplitude ratio of the cylinder under VIV, and the wake vortex shedding mode of the cylinder changes under this amplitude ratio.

Keywords: vortex-induced vibration; forced vibration; vortex shedding mode; amplitude ratio; frequency ratio

CLC number:U661.1

0 Introduction

Marine risers are mostly flexible pipes, which vibrate freely under the sea currents. However, due to the complex topology of the sea floor, the two ends of a certain riser laid on the sea floor are easily constrained, and a span is thus formed, and the riser will vibrate and cause damage under the sea currents. In research, this riser is usually considered as a rigid pipe elastically installed, and its hydrodynamic characteristics are studied by self-induced vibration or forced vibration [1-2].

Williamson et al. classified the structural patterns of the wake vortex shedding mode of vibrating risers through forced vibration experiments and divided different regions according to the vortex shedding modes [3]. Peppa et al. analyzed the energy transfer relationship between the incoming flow under low Reynolds numbers and riser structure and found that the wake vortex shedding mode was 2S at low dimensionless amplitude ratios (S indicates a single vortex shedding), and the mode gradually became complicated at high dimensionless amplitude ratios [4]. Meneghini et al. used the vibration frequency and amplitude of risers as variables, studied the wake vortex shedding frequency and the locking state of

Received: 2021 − 12 − 07 **Accepted:** 2022 − 02 − 17

Supported by: National Natural Science Foundation of China (52192692, 51639003, 52171294)

Authors: ZHOU Li, female, born in 1965, associate professor, master supervisor. Research interest: vortex-induced vibration, ship hydrodynamics. E-mail: zhouli@dlut.edu.cn

QIU Zhongqiu, male, born in 1995, master degree candidate. Research interest: computational fluid dynamics and ship hydrodynamics. E-mail: qzq2960@163.com

ZONG Zhi, male, born in 1964, Ph.D., professor, doctoral supervisor. Research interest: high-performance ships and ship hydrodynamics. E-mail: zongzhi@dlut.edu.cn

***Corresponding author:** QIU Zhongqiu

lateral vibrating risers at Re = 200, and identified the maximum amplitude value and variation range of vibration frequency when locking occurred at corresponding Reynolds numbers [5]. Morse et al. [6 - 7] discovered a new wake vortex shedding mode through experiments involving forced vibration and self-induced vibration of cylinders, and the mode belongs to the transition region of 2S and 2P modes (P represents a pair of vortex shedding with opposite rotation directions) and is defined as $2P_0$ mode.

Wang et al. [8] conducted a two-dimensional numerical simulation of the lateral forced vibration of cylinders in uniform flow (Re = 200) based on compact interpolation. Through the study on the sudden lift mutation of cylinders with lateral vibration in the constant flow, Zhu et al. [9] found that as the forced vibration amplitude increases, the pulsating lift coefficient of the cylinder will undergo a sudden decay, and under static condition, the vortex shedding frequency of the cylinder and the fluctuation controlled by the forced vibration frequency have a phase inversion, which makes the energy transfer between the cylinder and the fluid change reversely.

From the perspective of marine engineering applications, the study on forced vibration of elastically-supported risers aims to reveal the underlying laws of self-induced vibration and provide reliable experimental data for the prediction model of vortex-induced vibration (VIV) in marine risers [10]. In fact, most VIV predictors are corresponding prediction models based on a database obtained from forced vibration experiments, such as VIVANA and SHEAR7 [11-12], so as to meet the needs of engineering applications.

Self-induced vibration could intuitively reveal the phenomenon of VIV when the cylinder is subjected to a fluid force, but forced vibration could reveal the hydrodynamic characteristics under the interaction between fluid force and vibration at a deeper level [13]. There are great differences in the flow field changes and vibration responses between forced vibration and self-induced vibration, and little literature has involved in-depth research on the internal relationship between the two types of experiments. On this basis, this paper will integrate the numerical calculation of forced vibration and the experiment of self-induced vibration and link the dynamic response of forced vibration and the transition of vortex shedding mode with the maximum amplitude when the self-induced vibration encounters the locking state, in a bid to provide a reference for in-depth discussions of the relationship between the two.

1 Numerical model

1.1 Control equations

The flow field motion is simulated with a two-dimensional, incompressible, and viscous fluid, and its control equations, the Navier-Stokes system of equations, are represented in coordinate systems as

$$\frac{\partial u}{\partial x}+\frac{\partial v}{\partial y}=0 \tag{1}$$

$$\frac{\partial u}{\partial t}+u\frac{\partial u}{\partial x}+v\frac{\partial u}{\partial y}=-\frac{1}{\rho}\frac{\partial p}{\partial x}+\upsilon\left(\frac{\partial^2 u}{\partial x^2}+\frac{\partial^2 u}{\partial y^2}\right) \tag{2}$$

$$\frac{\partial v}{\partial t}+u\frac{\partial v}{\partial x}+v\frac{\partial v}{\partial y}=-\frac{1}{\rho}\frac{\partial p}{\partial y}+\upsilon\left(\frac{\partial^2 v}{\partial x^2}+\frac{\partial^2 v}{\partial y^2}\right) \tag{3}$$

where u and v are the components of fluid velocity in the x and y directions, respectively; p is the pressure; υ is the viscosity coefficient of fluid motion; ρ is the fluid density.

The solver used in this paper is the Realizable k-ε turbulence model in the STAR-CCM+ software. The standard k-ε model has advantages such as fast and stable calculation, as well as reasonable results, and thus it is suitable for calculating fluids of high Reynolds numbers. However, the model is not recommended for separated flow. The Realizable k-ε turbulence model proposed by Shih et al. [14] is an improved version of the standard k-ε model and could better simulate the boundary layer flow and separated flow with a strong pressure gradient. The transport equations of the turbulent kinetic energy and dissipation rate are as follows

$$\frac{\partial(\rho k)}{\partial t}-\nabla\cdot\left[\left(\mu+\frac{\mu_t}{\sigma_k}\right)\nabla k\right]+\nabla\cdot(\rho k u)=G_k+G_b-\rho\varepsilon-Y_M+S_K \tag{4}$$

$$\frac{\partial(\rho\varepsilon)}{\partial t}-\nabla\cdot\left[\left(\mu+\frac{\mu_t}{\sigma_\varepsilon}\right)\nabla\varepsilon\right]+\nabla\cdot(\rho k u)=\rho C_1 S_\varepsilon+C_{1\varepsilon}\frac{\varepsilon}{k}C_{3\varepsilon}G_b-\rho C_2\frac{\varepsilon^2}{k+\sqrt{\upsilon\varepsilon}}+S_\varepsilon \tag{5}$$

where u is the viscosity coefficient of dynamics; u_t is the turbulent viscosity; $C_1=\max\left[0.43,\frac{\eta}{\eta+5}\right]$, $\eta=\frac{S_k}{\varepsilon}$; $C_{1\varepsilon}=1.44$, $C_2=1.9$; σ_k and σ_ε are the turbulent Prandtl number of turbulent kinetic energy and dissipation rate of k and ε, respectively. σ_k equals 1.9, and σ_ε equals 1.2. G_k is the turbulent kinetic energy generation term caused by the average velocity gradient. G_b is the turbulent kinetic energy generation term caused by buoyancy. Y_M is the contribution rate of fluctuating expansion to the total dissi-

pation rate in compressible fluids. S_k and S_ε are user-defined source terms. $C_{3\varepsilon}$ equals zero, which indicates that the flow direction is perpendicular to the gravity direction.

1.2 Calculation domain and boundary conditions

The STAR-CCM+ software can effectively simulate the lateral forced vibration of a cylinder under a uniform incoming flow. First, the cylinder requires a subtraction operation, and different field functions are applied to the overlapping grids with the subtraction operation, so as to simulate the motion of the cylinder under different frequencies and amplitudes. The uniform flow velocity through the cylinder is U_0.

The calculation domain is shown in Fig. 1, in which the direction of the incoming flow velocity is parallel to the x axis, and the lateral vibration direction of the cylinder is parallel to the y axis. The diameter of the cylinder D equals 0.05 m, and its symmetrical boundaries are 20 D above and below the center of the cylinder. 20 D to the left of the center is the speed inlet, and 50 D to the right of the center is the pressure outlet. The cylinder surface is non-slip.

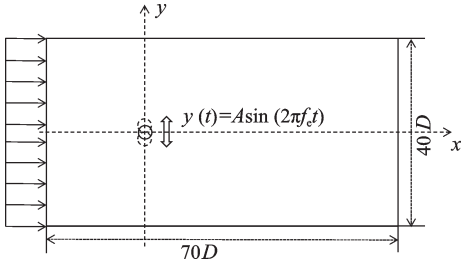

Fig. 1 Computational domain of cylinder's forced vibration

The cylinder conducts lateral forced vibration along the y axis, which is perpendicular to the direction of the incoming flow. The instantaneous displacement is

$$y(t) = A\sin(2\pi f_e t) \tag{6}$$

where A is the amplitude of the cylinder's lateral vibration, and f_e is the excitation frequency of the cylinder's forced vibration.

During the forced vibration, the instantaneous velocity of the cylinder in the y axis is

$$v_y(t) = 2\pi f_e A\cos(2\pi f_e t) \tag{7}$$

When the cylinder begins to vibrate, the instantaneous velocity $v_y(0)$ equals $2\pi f_e A$.

2 Verification of calculation feasibility

2.1 Verification of fixed cylinder

The meshing method and grid number directly affect the accuracy of the calculation results. To this end, the meshing method involving polygonal and prism layers is adopted. The extension area and rear area of the cylinder's lateral vibration are locally encrypted, and the overlapping grids which could cover the cylinder's motion are set around the cylinder, and the size of the overlapping area is $2D \times 5D$. The meshing method is shown in Fig. 2, and the calculation model is a structured grid with high accuracy. The wall-function method is used to perform near-wall treatment on the cylinder's surface, and grids in the first layer of the surface meet the condition of $y+ \approx 1$. With Re = 20 000, the incoming flow velocity U_0 equals 0.356 m/s. If the density of the fluid is 997 kg/m^3, and the dynamic viscosity is 0.895×10^{-3} kg/(s·m), the thickness of the grids in the first layer adjacent to the surface Δs equals 0.04 mm through calculation. If the number of prism layers n equals 10, and the growth rate q is 1.3, according to $\delta = (\Delta s(1-q^n))/(1-q)$, the total thickness of the boundary layer is 1.67 mm.

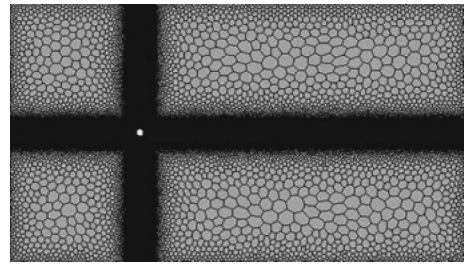

Fig. 2 Meshing of fixed grids

The irrelevance of the grid and time step size is verified. While ensuring the accuracy of calculation, the paper saves the cost, and the final number of grids is 390 000, and the time step size is 0.01 s. In order to verify the reliability of the calculation model, the winding problem of fixed and vibrating cylinders in the uniform flow of Re = 20 000 is numerically calculated, as shown in Fig. 3, and the characteristic frequency of vortex shedding of the cylinder is determined to be 1.46 Hz by observing the curve of energy spectrum density of the lift coefficient.

According to the formula

$$S_t = \frac{f_{ov} \cdot D}{U_0} \tag{8}$$

where f_{ov} is the wake vortex shedding frequency of

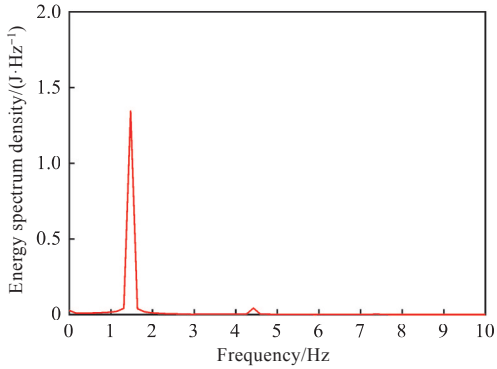

Fig. 3 Energy spectrum density of lift coefficient of fixed cylinder with Re = 20 000

the cylinder, and the Strouhal number S_t = 0.204 8 of the fixed cylinder with Re = 20 000 can be obtained, which is basically consistent with S_t = 0.2 in literature [15].

2.2 Calculation of forced vibration of the cylinder

The numerical calculation of forced vibration of the cylinder under the same incoming flow conditions was performed. The results obtained at A/D = 0.5 and a frequency ratio of forced vibration of $0.5 \leqslant f_e/f_s \leqslant 1.5$ (f_s is the Strouhal frequency) are compared with the numerical results by Yu et al. [16] and the experiment results by Sarpkaya [17]. As can be seen from Fig. 4, the calculation results of this paper are consistent with the trend of change in the amplitude of the maximum lift coefficient in literature [16 - 17]. As the frequency ratio increased, the curves showed an increasing trend and leaped around f_e/f_s = 1 [18 - 19]. Due to the difference between the corresponding Reynolds numbers in this paper and the reference condition, as well as the difference in the corresponding frequency ratio, the result is biased and consistent with the actual situation. The example above verified that the proposed model could be used to solve the problem of forced vibration of cylinders under sub-critical Reynolds numbers.

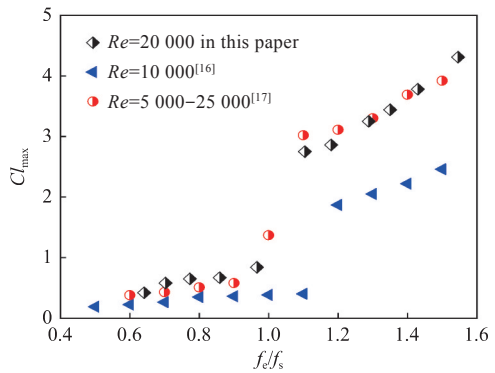

Fig. 4 Variation of Cl_{max} with f_e/f_s at A/D = 0.5

3 Analysis of calculation results

3.1 Numerical analysis of forced vibration

This paper adopts the method of external excitation to make the cylinder perform self-induced vibration-like motion under the uniform flow. By controlling A and f_e, the time-domain curve of the cylinder's displacement shows a simple harmonic motion pattern. The dimensionless amplitude ratio A/D and the excitation frequency ratio f_e/f_n are shown in Table 1 (f_n is the natural frequency of the structure, which takes into account the additional water mass). A threshold for the corresponding amplitude appears when VIV reaches the locking state [3], and the minimum A/D is 0.3. f_n = 0.714 2 Hz was obtained from free attenuation vibration experiments.

Table 1 Dimensionless frequency ratio and amplitude ratio

A/D	f_e/f_n
0.3~1.2	0.83，0.91，1.00，1.11，1.25，1.42

Since the cylinder is subjected to the dual action of the fluid force and the excitation force during forced vibration, it is assumed that the lift obtained in the numerical calculation is F_m, and the lift provided by the fluid force is F_l. The effect of forced vibration on the lift of the cylinder is expressed by inertia force F_i. The relationship between the three can be expressed by Eq. (9):

$$F_m = F_l + F_i \tag{9}$$

When the directions of F_l and F_i are the same, F_m is greater than F_l. When the direction of F_l is opposite to that of F_i, F_m is smaller than F_l. When the cylinder is fixed, i.e., A/D = 0, F_i equals zero, and F_m equals F_l. In addition, when the vibration velocity of the cylinder reaches the maximum value, which means that the vibration acceleration is zero, F_i equals zero, and F_m equals F_l. It can be seen that when the vibration velocity of the cylinder reaches its maximum during a single vibration cycle, the measured lift is provided only by the fluid force.

Fig.5 shows the curve of the vibration velocity v_y and the corresponding lift coefficient Cl curve in a single cycle under different amplitude ratios and f_e/f_n = 0.83. As can be seen from the figure, the vibration velocity curve always follows the pattern of simple harmonic motion, but due to the influence of inertia force by forced vibration, the lift coefficient curve in a single cycle does not change regularly.

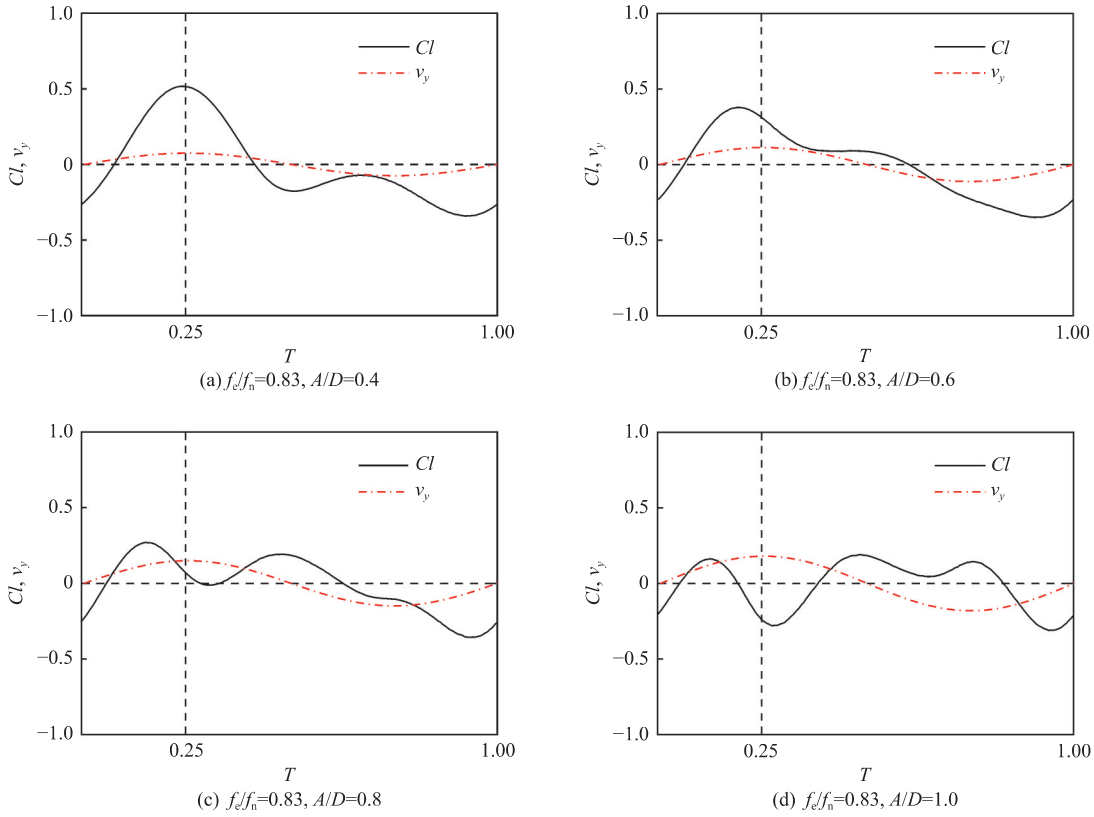

(a) f_e/f_n=0.83, A/D=0.4 (b) f_e/f_n=0.83, A/D=0.6

(c) f_e/f_n=0.83, A/D=0.8 (d) f_e/f_n=0.83, A/D=1.0

Fig. 5 Vibration velocity and lift coefficient curve in a single cycle

When A/D is large enough, it can be observed that the lift coefficient curve contains multiple peaks in a single cycle.

Meanwhile, it can be found that as A/D increases, in the rising stage of the cylinder (0−0.5T), the lift coefficient value corresponding to the maximum vibration velocity (0.25T) will change from positive to negative. In the declining stage (0.5T−T), the lift coefficient value corresponding to the maximum vibration velocity (0.75T) will change from negative to positive. In the study of forced vibration, the lift coefficient of the fixed cylinder (A/D = 0) is usually positive. Therefore, at the end approaching A/D = 0, the lift coefficient should be positive. In the numerical calculation of the forced vibration in this paper, the position (0.25T) where the vibration velocity of the cylinder reaches the maximum in the rising stage is selected as the lift coefficient monitoring position.

Fig.6 is a conservative model in the VIV predictor SHEAR7, where the Cl−A/D curve under different dimensionless frequency ratios is usually obtained by data points (0, Cl_0), ((A/D)*, Cl_{max}), and ((A/D)max, 0) through quadratic function fitting, where (A/D)* and $(A/D)_{max}$ represent the dimensionless amplitude ratio [19] when the lift coefficient is zero and maximum, respectively. In the model, Cl rises first and then decreases as A/D increases, and meanwhile, it gradually changes from positive to negative.

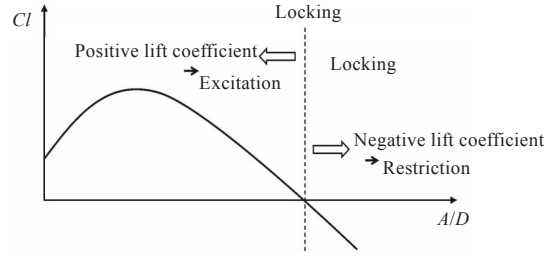

Fig. 6 Variation of Cl with dimensionless A/D

Fluid forces can improve the amplitude of the cylinder, while vibration can prevent the amplitude of the cylinder from increasing [20]. Under their interaction, when the lift coefficient is positive, it means that the vibration has a limited ability to constrain the fluid force. If the incoming flow velocity continues to increase at this time, the riser's amplitude can still enhance, which indicates that the amplitude of the cylinder will increase as the incoming flow velocity rises when the VIV does not reach the locking state. As the amplitude ratio increases, the vibration's ability to constrain the fluid force is further enhanced until the lift coefficient at the equilibrium position is zero. At this time, the two forces are balanced, and the amplitude reaches the maximum and no longer increases. It is worth mentioning that in VIV, the restriction effect of the vibration

will not exceed the excitation effect of the fluid force. In other words, the lift coefficient will never be negative. Therefore, when the locking state is reached, as flow velocity varies within a certain range, the amplitude of the cylinder can still remain unchanged at the maximum value even if the flow velocity is increased.

The forced vibration of the cylinder occurs under external excitation. By changing A/D, the paper observes the lift coefficient at the monitoring position and fits the variation curve of the Cl with A/D under different f_e/f_n. By conducting third-order polynomial fitting of the numerical calculation results under each working condition, as well as controlling the fitting condition of Cl_0 = 0.168 (the lift coefficient of the fixed cylinder at Re = 20 000), the paper obtains a fitted curve. By inputting relevant parameters and conditions in SHEAR7, the paper can also obtain a predicted fitted curve. Two fitted curves under the same frequency ratio are compared and analyzed, and the results are shown in Fig. 7.

As can be seen from Fig. 7, the fitted curve of the numerical calculation results obtained under different excitation frequencies is highly consistent with the SHEAR7 fitted curve, which indicates that the lift coefficient rises first and then falls as A/D increases. The traditional methods for the lift coefficient in the calculation of forced vibration often fail to show this trend, and this indicates that the lift coefficient selected at the maximum vibration velocity in the rising stage is suitable for establishing a VIV prediction model.

To further understand the relationship between the fitted curve of the numerical calculation results and the amplitude response of the VIV, the zero-lift coefficient point near f_e/f_n = 1 is analyzed. As shown in Fig. 8, the zero-lift coefficient point at the equilibrium position remains around A/D=0.8. Through comparative analysis with the SHEAR7 prediction model, it can be seen that the maximum amplitude should remain around 0.8D when the VIV reaches the locking state under the sub-critical Reynolds numbers. As a result, the maximum amplitude response of the cylinder under a self-induced frequency ratio $f_{ov}/f_n \approx 1$ can be predicted, and f_{ov} is the wake vortex shedding frequency of the cylinder during self-induced vibration.

According to Fig. 8, under the same amplitude ratio, the lift coefficient gradually increases as the frequency ratio rises. When f_e/f_n equals 1.42, the lift coefficient is greatly increased compared with other groups, and a burst occurs [12]. The relevant mechanism needs to be further explored.

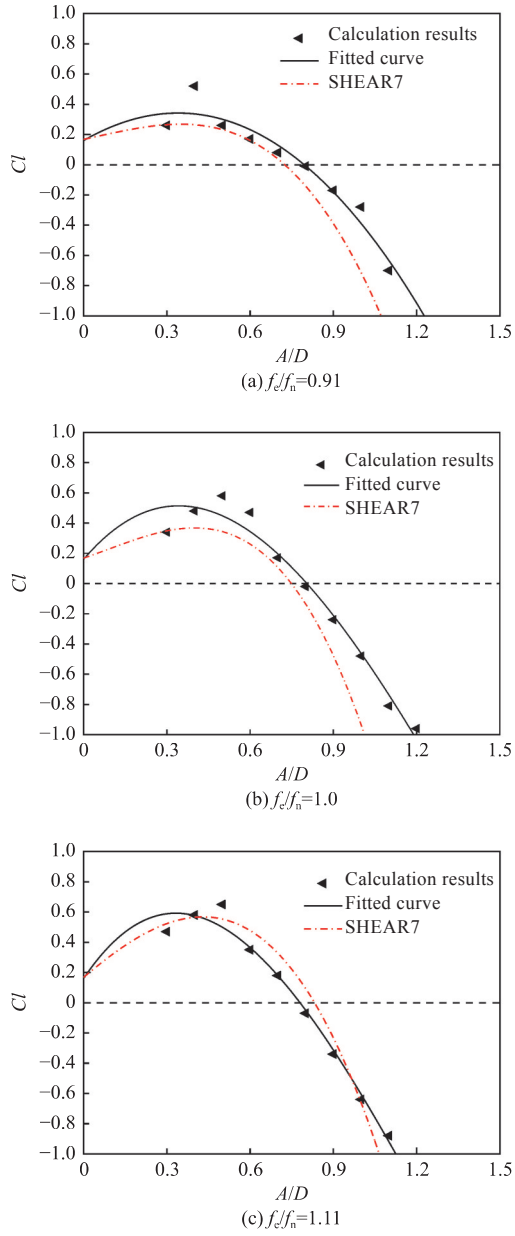

Fig. 7 Fitted curves of lift coefficient under different excitation frequencies

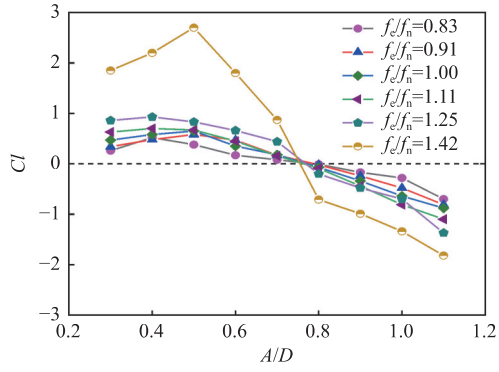

Fig. 8 Variation of Cl with A/D under different working conditions

3.2 Comparative analysis of self-induced vibration experiments

The numerical calculation of forced vibration shows that the corresponding amplitude ratio is maintained at around 0.8 when the lift coefficient at the monitoring position is zero. Under self-induced vibration, the maximum amplitude of VIV of the cylinder elastically installed at the sub-critical Reynolds number is predicted to be around 0.8D, and it is in a locking state at this time ($f_{ov}/f_n \approx 1$). In order to verify the prediction results, self-induced vibration experiments were designed and performed.

Fig. 9 shows an experimental device for self-induced vibration, in which the vibrating cylinder is embedded in the vibrating frame and elastically installed on a fixed device. The spring has a certain spring coefficient, and the vibrating frame can drive the cylinder to do vertical and reciprocating motion along the slide rails on both sides. In order to minimize the three-dimensional effect, the ports of the U-shaped frame at both ends of the fixed cylinder use thin and light plates. The diameter of the cylinder used in the experiment is consistent with that in the numerical calculation. The spring coefficient K equals 230.48 N/m, and the velocity of the uniform incoming flow ranges from 0.13 to 0.34 m/s. The corresponding reduction velocity U_r varies within 3.7−9.4 m/s.

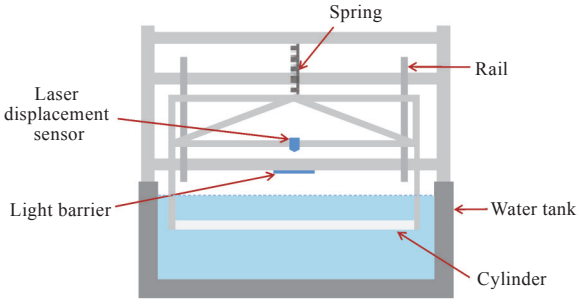

(a) Diagram of experimental device for VIV

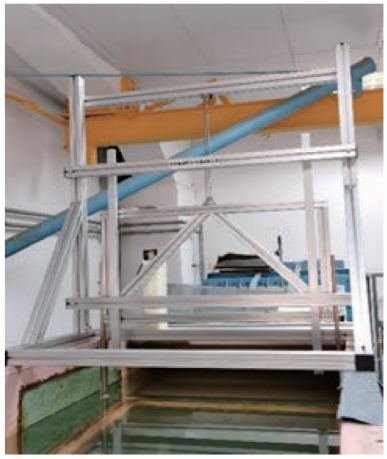

(b) Experimental device for VIV

Fig. 9 Experimental device for VIV

By changing the velocity of incoming flow, the vibration amplitude of the cylinder and the corresponding f_{ov}/f_n are monitored, and the maximum amplitude of the vibrating cylinder and the corresponding frequency ratio range in the locking state can be observed. Fig. 10 shows the change in A/D and f_{ov}/f_n with U_r in a self-induced vibration experiment. As can be seen from the figure, when f_{ov}/f_n is close to 1, the amplitude ratio is greatly increased. In a certain f_{ov}/f_n range, A/D does not change greatly, which indicates a locking state. At the same time, it can be observed that the reduction velocity corresponding to the locking range makes the maximum amplitude of the cylinder reach about 0.8 D.

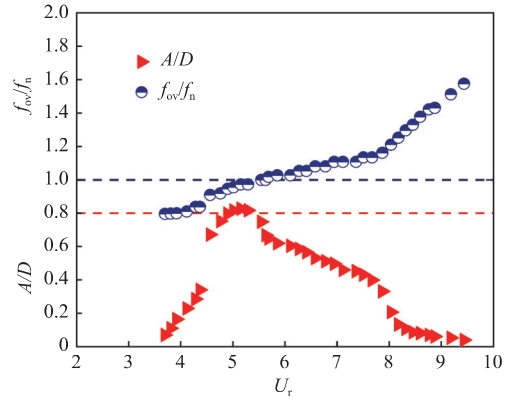

Fig. 10 Variation of amplitude ratio and self-induced vibration frequency ratio of cylinder with different reduction velocity

3.3 Analysis of vortex shedding mode transition

Williamson et al. [3] conducted experimental studies on the wake vortex shedding modes of a vibrating cylinder, defined different regions according to the structural forms of wake vortex shedding, and found that the main vortex shedding modes near the locking region are 2S, 2P, and P+S. As the dimensionless amplitude ratio increases, there is usually a transition from 2S mode to P+S or 2P mode near the critical line of vortex shedding mode transition. Experimental studies have shown that at low Reynolds numbers (Re < 300), the P+S mode will replace the 2P mode so that only the P+S mode occurs in the whole region. At larger Reynolds numbers, the boundary between the P+S and 2P modes is basically the same as the critical line of transition. It can be seen that as the Reynolds number changes, it is not clear if the 2P mode or P+S mode will appear after the vortex shedding mode in the same region changes, but the critical line of the transition remains basically unchanges.

Under the same forced vibration frequency ratio, the vorticity of the same time in the range of A/D = 0.6−1.0 is selected. As shown in Fig. 11, the amplitude ratio under different frequency ratios increases sequentially from 0.6 to 1.0. It can be found that when the amplitude ratio is less than 0.8, such as the vortex pair marked by the red coil at A/D 0.7, the wake vortex shedding of the cylinder is the P+S mode. When the amplitude ratio is greater than 0.8, such as the vortex pair marked by the red coil at A/D=0.9, the wake vortex shedding is the 2P mode. This implies that in the forced vibration, A/D = 0.8 is the critical line for the transition of the wake vortex shedding mode, and the zero-lift coefficient point of the monitoring position appears at the same time as the wake vortex shedding mode changes.

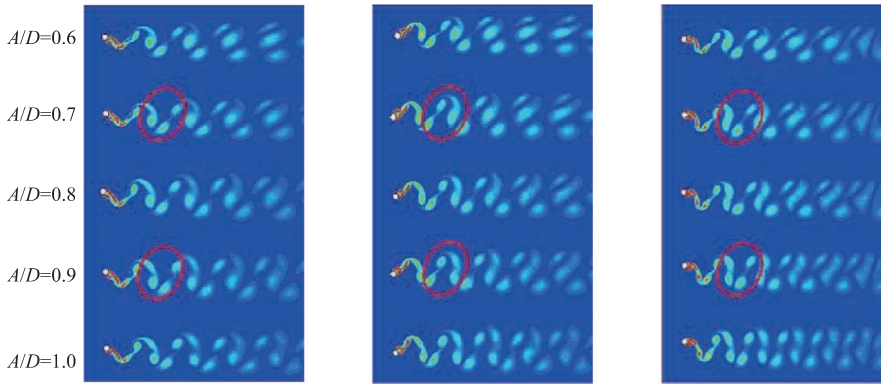

Fig. 11 Variation of vorticity under different frequency ratios with amplitude ratio

4 Conclusions

In this paper, the position for selecting the response value of the lift coefficient during the forced vibration of the cylinder is studied, and the relevant mechanism is analyzed. The maximum amplitude of the VIV when the cylinder reaches a locking state is predicted and verified through comparison, and the transition of the vortex shedding mode when the lift coefficient at the equilibrium position is zero is discussed. Through the analysis, the following conclusions are drawn:

1) The response of the lift coefficient when the cylinder has a forced vibration under the sub-critical Reynolds numbers is quite different from that of self-induced vibration. When the cylinder velocity reaches the maximum during the forced vibration, the monitored lift is only provided by the fluid force, and it is reasonable to take the lift coefficient corresponding to the maximum vibration velocity (0.25T) of the cylinder in the rising stage as the calculation result.

2) The fitted curve of the numerical simulation result is in good agreement with the relevant fitted curve by the VIV predictor SHEAR7, and their changes remain highly consistent. Their lift coefficients both increase first and then decrease as the amplitude ratio rises, which provides a method for predicting the amplitude response of the VIV by establishing a Cl-A/D model according to the numerical result of the forced vibration.

3) The numerical calculation results show that the zero-lift coefficient points at the equilibrium position of the cylinder during the forced vibration are maintained near A/D = 0.8, and the prediction results are compared and verified by the self-induced vibration experiments. Experimental results show that when f_{ov}/f_n is closer to one, the amplitude ratio increases significantly, and as f_{ov}/f_n varies within a certain range, A/D does not change significantly, which indicates that the locking state is reached. Meanwhile, the maximum amplitude of the cylinder in the locking state is about 0.8D, which proves that the prediction method is feasible.

4) The zero-lift coefficient at the equilibrium position and the corresponding wake vortex shedding mode of the cylinder are discussed. The calculation results show that when the amplitude ratio is less than 0.8, the wake vortex shedding mode is the P + S. When the amplitude ratio is greater than 0.8, the wake vortex shedding mode is the 2P. The amplitude ratio corresponding to the zero-lift coefficient of the Cl-A/D curve of the forced vibration is basically the same as the maximum response amplitude ratio when the cylinder reaches the locking state during VIV, and the wake vortex shedding mode changes at this amplitude ratio.

In the future, the frequency ratio interval in which the cylinder will reach a locking state under uniform incoming flow can be predicted by calculat-

ing the cylinder vibration under different Reynolds numbers.

References

[1] WILLIAMSON C H K, GOVARDHAN R. Vortex-induced vibrations [J]. Annual Review of Fluid Mechanics, 2004, 36 (1): 413−455.

[2] HOU L, DING Y F, WANG Q, et al. Prediction method of hydrofoil vortex shedding frequency at high Reynolds numbers [J]. Chinese Journal of Ship Research, 2019, 14 (6): 88−97 (in Chinese).

[3] WILLIAMSON C H K, ROSHKO A. Vortex formation in the wake of an oscillating cylinder [J]. Journal of Fluids and Structures, 1988, 2 (4): 355−381.

[4] PEPPA S, KAIKTSIS L, TRIANTAFYLLOU G S. Hydrodynamic forces and flow structures in flow past a cylinder forced to vibrate transversely and inline to a steady flow [J]. Journal of Offshore Mechanics and Arctic Engineering, 2016, 138 (1): 011803.

[5] MENEGHINI J R, BEARMAN P W. Numerical simulation of high amplitude oscillatory flow about a circular cylinder [J]. Journal of Fluids and Structures, 1995, 9 (4): 435−455.

[6] MORSE T L, WILLIAMSON C H K. Fluid forcing, wake modes, and transitions for a cylinder undergoing controlled oscillation [J]. Journal of Fluids and Structures, 2009, 25 (4): 697−712.

[7] MORSE T L, WILLIAMSON C H K. Prediction of vortex-induced vibration response by employing controlled motion [J]. Journal of Fluid Mechanics, 2009, 634: 5−39.

[8] WANG K P, ZHAO X Z. Research about lift and drag coefficient of circular cylinder oscillating transverse to the flow [J]. Journal of Jiangsu University of Science and Technology (Natural Science Edition), 2017, 31 (5): 579−585 (in Chinese).

[9] ZHU Y J, ZONG Z. Study on the sharp change of lift force of a cylinder with transverse vibration in the steady flow [J]. Chinese Journal of Hydrodynamics, 2020, 35 (5): 592−600 (in Chinese).

[10] DENG D, WANG Z, WANG D C. Numerical simulation of vortex-induced vibration of a 2D cylinder in oscillatory flow [J]. Chinese Journal of Ship Research, 2018, 13 (Supp 1): 7−14 (in Chinese).

[11] WU J, M. LEKKALA K R, ONG M C. Numerical investigation of vortex-induced vibrations of a flexible riser with staggered buoyancy elements [J]. Applied Sciences-Basel, 2020, 10 (3): 905.

[12] VANDIVER J K, LI L. SHEAR7 program theory manual [M]. [S. l.]: Department of Ocean Engineering, MIT, 1999.

[13] DUAN J L, ZHOU J F, WANG X, et al. Cross-flow vortex-induced vibration of a flexible riser with internal flow in shear current [J]. Chinese Journal of Theoretical and Applied Mechanics, 2021, 53 (7): 1876−1884 (in Chinese).

[14] SHIH T H, LIOU W W, SHABBIR A, et al. A new k-ε viscosity model for high Reynolds number turbulent flows [J]. Computers & Fluids, 1995, 24 (3): 227−238.

[15] DENG Y. Study on forced oscillation and vortex-induced vibration (VIV) of circular cylinder under combined uniform flow and oscillatory flow at low Reynolds number[D]. Qingdao: Ocean University of China, 2014 (in Chinese).

[16] YU C X, WANG J S, ZHENG H X. Two-dimensional simulation on forced oscillations of a circular cylinder using high-resolution TVD-FVM method [J]. Chinese Journal of Hydrodynamics, 2018, 33 (5): 593−600 (in Chinese).

[17] SARPKAYA T. Hydrodynamic damping, flow-induced oscillations, and biharmonic response [J]. Journal of offshore Mechanics and Arctic engineering, 1995, 117 (4): 232−238.

[18] GOPALKRISHNAN R. Vortex-induced forces on oscillating bluff cylinders [D]. Cambridge: Massachusetts Institute of Technology, 1993.

[19] FAN J J, TANG Y G, ZHANG R Y, et al. Numerical simulation of viscous flow around circular cylinder at high Reynolds numbers and forced oscillating at large ratio of amplitude [J]. Chinese Journal of Hydrodynamics, 2012, 27 (1): 24−32 (in Chinese).

[20] PARK K S, KIM Y T, KIM D K, et al. A new method for strake configuration design of Steel Catenary Risers [J]. Ships and Offshore Structures, 2016, 11 (4): 385−404.

亚临界雷诺数下单圆柱涡激振动研究

周力，邱中秋*，袁亚帅，宗智

大连理工大学 船舶工程学院，辽宁 大连 116024

摘　要：［**目的**］为了实现亚临界雷诺数下圆柱涡激振动振幅响应的准确预报，利用数值模拟方法研究强迫振动时圆柱的升力系数与振幅比（*Cl*-*A*/*D*）之间的关系。［**方法**］基于Realizable k-ε 湍流模型，采用有限体积法对圆柱的强迫振动进行二维数值模拟，计算得到激振频率比f_e/f_n=1 附近范围内不同振幅比下的升力系数曲线。选取圆柱振动速度最大时对应的升力系数，建立 *Cl*-*A*/*D* 关系曲线。［**结果**］结果表明，*Cl*-*A*/*D* 拟合曲线总体变化趋势与涡激振动预报程序SHEAR7 的结果吻合良好。同时，各激振频率比 fe/fn 下的零升力系数点均位于振幅比 *A*/*D*=0.8 附近，且结构尾涡脱落模式在 *A*/*D*=0.8 附近发生了转变，由“P+S”模式转变到“2P”模式（P表示一对旋转方向相反的旋涡脱落，S 表示单个旋涡脱落）。在圆柱涡激振动实验中，发现涡激振动出现“锁定”时的最大振幅在0.8*D* 附近。［**结论**］亚临界雷诺数下强迫振动圆柱 *Cl*-*A*/*D* 关系曲线升力系数为零时对应的振幅比与圆柱在涡激振动中的最大响应振幅比基本保持一致，且圆柱尾涡脱落模式在此振幅比下发生了转变。

关键词：涡激振动；强迫振动；涡脱模式；振幅比；频率比